TELKOMNIKA Indonesian Journal of Electrical Engineering
Vol.12, No.5, May 2014, pp. 3444 ~ 3459
DOI: http://dx.doi.org/10.11591/telkomnika.v12i5.5362

A Lyapunov Approach to Control Design for Grid-connected Inverters

Vu Tran, **Mufeed MahD***
Department of Electrical Engineering, University of Massachusetts, Lowell
Ball Hall 321, 1 Unviersity Ave. Lowell, MA, 01854, USA
*Corresponding author, e-mail: mufeed mahd@uml.edu

Abstract

This paper develops a Lyapunov approach to control design for grid connected inverter. The control objective is to track a reference current which is proportional to the fundamental harmonic of the grid voltage. By using the internal model principle, the grid voltage and the reference current are described as the outputs of an autonomous linear oscillatory system. The state of this oscillatory system contains all the information for the harmonics of the grid voltage and is estimated via an observer wit zero estimation error at steady state. A state space description for the whole system is obtained by combining the state of the inverter circuit and that of the oscillatory system for the grid voltage. Based on the state space description, a Lyapunov approach is developed to design a state-feedback controller for tracking a reference current with minimal tracking error. The design problem is cast into an optimization problem, which can be effectively solved with linear matrix inequality (LMI) toolbox in Matlab. The Lyapunov approach ensures internal stability and makes efficient use of the structural information, such as the total harmonic distortion (THD) of the grid voltage, and the magnitude/phase of the reference current. The effectiveness of the Lyapunov approach is validated via SimPower simulation. A real circuit is built using microcontroller ezDSP28335, the output current obtained is in phase with the grid voltage and has small THD, as we expected.

Keywords: *grid-connected inverter, state-space description, total harmonic distortion (THD), linear matrix inequalities, Lyapunov approach*

1. Introduction

As the demand for power is increasing significantly, renewable energy sources have recently received a lot of attention as an alternatives way of generating directly electricity. Using renewable energy systems can eliminate harmful emissions from polluting the environment while also offering inexhaustible resources of primary energy. There are many sources of renewable energy, such as solar energy, wind turbines, water turbines, and geothermal energy. However, solar and wind energy system make use of advanced power electronics. Most of the renewable energy technologies produce direct current (DC) power and hence inverters are required to convert the DC to the alternating current (AC) power. There are two kinds of inverters: Stand-alone (island) and grid-connected. These two types have several similarities, but are different in terms of control function. A stand-alone inverter is used in off grid applications. The generated power from renewable energy is delivered to loads, or can be stored in batteries. But that kind of systems requires complexity and high maintenance, such that rechargeable batteries. That also increases the size and cost for the system. Grid-connected inverters overcome this limitation. For gridconnected inverters, they must follow the voltage and the frequency characteristics of the utility generated power presented on the distribution line. The main advantage of this system is that no battery is required for storing the energy from renewable sources, which reduces the size and cost of the system. Moreover, it is easier to create a portable inverter due to the compact size of the system. Investigations of different configurations and control methods for grid-connected inverters are being developed in recent years. A comprehensive review of single-phase grid-connected inverters [1] has covered some of the standards that inverters for grid applications must be fulfilled, such as the standards EN61000-3-2, and the U.S National Electrical Code (NEC) 690. It also provided a classification of the inverters regarding the stage (single, dual stage, and multi-string inverter), transformers

Received November 14, 2013; Revised December 7, 2013; Accepted December 27, 2013

and types of Interconnections, and types of grid interfaces (line-commutated current-source inverter and self-commutated voltage-source inverter). Three-Phase Grid-Connected inverters were presented in [2, 3]. The combination of island mode and grid-connected mode was investigated in [4, 5]. In grid-connected mode, inverter operates in connection with the grid. When disconnected from the grid, the inverter should be automatically disconnected from the utility grid and changed to island mode in order to ensure the continuous power supply for the load from the inverter [6]. A main problem which needs much effort in power inverters these days is reducing the harmonics. The IEEE 929 standard stated that the Total Harmonic Distortion (TDH) of voltage and current should be lower than 5% in normal operation. Harmonics are not desirable because they cause overheating, decreased voltampere capacity, increased losses, distorted voltage and current waveform, etc. There are two sources of harmonics: one is from the inverters (due to the pulse width modulation and the switching), and the other is from loads or grid. These harmonic currents then cause distortion in the voltage because of the impedances in the distribution network and inside the voltage source. And the harmonics in voltage can cause harmonics in current as well. Several researches have been proposed to reduce the voltage THD of inverters. For example, the repetitive control theory has been successfully applied to PWM inverters [7-14], active filters [15-17], dead-beat control [18, 19], to reduce THD. Harmonic droop control technique [20] is also presented. Repetitive control has an excellent ability in eliminating periodic disturbances, however, in practical, this technique is limited in slow dynamics, poor tracking accuracy, and poor performance to non-periodic disturbances. Dead-beat and sliding-mode controls have excellent dynamic performance in control of output voltage, but these techniques suffer from complexity, sensitivity, and steady-state errors In order to eliminate the current distortion, some current control methods are proposed, such that proportional resonant controller and multi-resonant controllers in [21], active power filters in [17, 22]. A promising control techniques in grid-connected inverter is output current tracking. The inverter's current polarity must be taken care of, to match the voltage polarity of the grid. Various synchronization methods are summarized in [23-25]. The current hysteretic comparison control method, timing control of current instantaneous comparison method and the triangle wave comparison control method of timing tracking current are proposed in [26]. In [27], algorithms of current decoupling are derived for performing the reactive power control of grid-connected inverter. Through zero-crossing detecting circuit in [28] and [29], the inverter is controlled so as to generate the output current in phase with the grid voltage. A current control employing internal model principle in [30] is proposed to suppress the harmonic currents injected into the grid. Although most existing controllers give satisfactory results, the theory behind the dynamics and performances is not clearly described. The purpose of this paper is to develop a systematic state space approach so that the dynamics of the whole system can be more clearly understood. A simple feedback law is designed to track a reference current with minimal tracking error. The design problem will be investigated using advanced nonlinear control system theory and linear matrix inequality (LMI) optimization technique, as in [31-35]. The problem of tracking current error will be casted into Lyapunov framework, which ensures internal stability and the total harmonics distortion (THD) requirements. The paper is organized as follows. Section II describes the open loop description for the inverter circuit, following is the state-space description for the grid voltage and an observer, and control objective. Section III reviews the main tool to be used in this paper - Lyapunov approach to evaluation of the tracking error. Section IV casts the problem of tracking error into Lyapunov framework and converts the designproblem into the LMI optimization. Section V uses SimPower in MATLAB to simulate and verify the results. Section VI uses experiment results to validate the design method. Section VII concludes the paper.

2. State Space Description of the Inverter and Control Objective

2.1. Open-loop Description for the Inverter Circuit

Figure 1 is the equivalent circuit of a grid-connected inverter, where *vg* is the grid voltage. The input voltage *u* is actually the output of the transistor bridge, which is driven by a pulse-width-modulated (PWM) signal. For simplicity, the transistor bridge is not included.

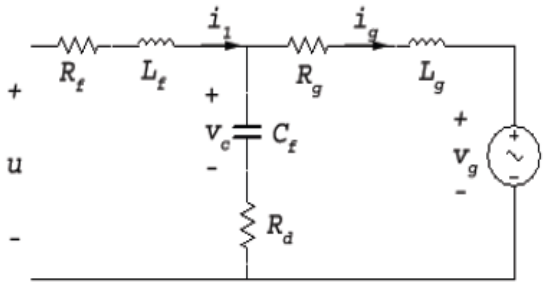

Figure 1. Equivalent Circuit for a Grid-connected Inverter

Let the duty cycle of the PWM signal be *d* and the DC voltage supply be *Vs*. Under the assumption of ideal switching, when PWM signal is in the ON state, *uON* = *Vs*, and when PWM signal is in the OFF state, *uOFF* = −*Vs*. Under the assumption of high frequency, the input signal *u* can be averaged from *uON* and *uOFF* over one switching period, *u* = *dVs* + (1 − *d*)(−*Vs*) = (2*d* − 1)*Vs*. Thus we call the simplified circuit of the averaged model for the inverter, and *u* can be considered as the input.

Let the state of the circuit as:

$$x_c = \begin{bmatrix} v_c \\ i_1 \\ i_g \end{bmatrix}$$

Define:

$$A = \begin{bmatrix} 0 & \frac{1}{C_f} & -\frac{1}{C_f} \\ -\frac{1}{L_f} & -\frac{R_f+R_d}{L_f} & \frac{R_d}{L_f} \\ \frac{1}{L_g} & \frac{R_d}{L_g} & -\frac{R_d+R_g}{L_g} \end{bmatrix}$$

$$B = \begin{bmatrix} 0 \\ \frac{1}{L_f} \\ 0 \end{bmatrix}, \quad E = \begin{bmatrix} 0 \\ 0 \\ -\frac{1}{L_g} \end{bmatrix}$$

The circuit can be described as:

$$\dot{x_c} = Ax_c + Bu + Ev_g \tag{1}$$

Where *u* is the control input and *vg* can be considered as an external disturbance.

2.2. State-space Description for the Grid Voltage and an Observer

The grid voltage is periodic with frequency 50Hz or 60Hz. The frequency may subject to some perturbation but can be measured. Let the fundamental frequency be *β*0 (rad/second). According to [36], the grid voltage *vg*(*t*) can be expressed as a Fourier series:

$$v_g(t) = \sum_{k=1}^{\infty} b_k \sin(k\beta_0 t + \phi_k) \tag{2}$$

The magnitude *bk* and the phase *ϕk* for each harmonic can be evaluated with a bank of resonant filters [21], [37-38], or a composite observer [39, 40]. The resonant filters are described with transfer functions, while the composite observers are described via state-space equations. They are all based on the internal model principle in [41, 42]. Here we adopt the main ideas in [40] to describe *vg* via state space equations and then construct an observer to estimate the state. The advantage of using the state space description is that the dynamics of the whole

system can be simply described by stacking up the state equation for *vg* and that for the circuit, i.e., (1). The resulting state equation for the whole system makes it very convenient to study the interaction between the grid voltage and the dynamics of LCL filter. Furthermore, it facilitates analysis of system performance via advanced tools developed in recent years, such as the Lyapunov approach and the linear-matrix-inequality (LMI) based optimization.

We may consider *vg*(*t*) as a disturbance with known frequency for the harmonics but uncertain magnitude and phases. This type of disturbances can be modeled as the output of a linear time invariant system, as in [31] and [41]. Let:

$$v_{g1}(t) = b_1 sin(\beta_0 t + \phi_1)$$

Denote:

$$S_0 = \begin{bmatrix} 0 & -\beta_0 \\ \beta_0 & 0 \end{bmatrix}$$
$$\Gamma = [1 \quad 0]$$

Then *vg*1(*t*) is the output of the following 2*nd* order linear system.

$$\dot{w}_g = S_0 w_g, \quad v_{g1} = \Gamma w_g, \quad w_g(0) = w_{g0} = \begin{bmatrix} b_1 sin\phi_1 \\ b_1 cos\phi_1 \end{bmatrix} \tag{3}$$

We may include more harmonics by simply increasing the size of S with more diagonal blocks of the form $kS_0 = \begin{bmatrix} 0 & -k\beta_0 \\ k\beta_0 & 0 \end{bmatrix}$ and increasing the dimension of *wg*.

Define:

$$S_g = \begin{bmatrix} S_0 & 0 & \cdots & 0 & 0 \\ 0 & 2S_0 & \cdots & 0 & 0 \\ \vdots & \vdots & \ddots & \vdots & \vdots \\ 0 & 0 & \cdots & (N-1)S_0 & 0 \\ 0 & 0 & \cdots & 0 & NS_0 \end{bmatrix}$$

Where 0's in the above matrix are all 2 by 2 blocks. Also define:

$$\Gamma_g = [1 \quad 0 \quad 1 \quad 0 \quad \cdots \quad 1 \quad 0]$$

Then *vg* is the output of the following autonomous linear oscillatory system:

$$\dot{w}_g = S_g w_g, \qquad v_g = \Gamma_g w_g$$

Where *wg* ∈**R**2*N*. A prominent feature of the matrix *Sg* is that $S_g + S_g^T = 0.$ Because of this, we have *wg*(*t*)*Twg*(*t*) = *wg*(0)*Twg*(0) = ∥*wg*(0)∥2 for all *t*. This kind of state-space descriptions for periodic signals has been widely used in the output regulation literature for tracking periodic references or rejection of periodic disturbances [31-[33], [41], where the linear system (4) was referred to as the exogenous system, or simply, exosystem.

The state *wg* ∈**R**2*N* can be decomposed as:

$$w_g = [w_{g1}^T \quad w_{g2}^T \quad \ldots \quad w_{gN}^T]^T$$

where *wgk* ∈**R**2, *k* = 1, . . . , *N*. By the structure of Γ*g*, we have $v_g(t) = \sum_{k=1}^{N} [1 \quad 0] w_{gk}(t)$. Furthermore $[1 \quad 0] w_{gk}(t) = b_k \sin(k\beta_0 t + \phi_k)$ is exactly the *kth* harmonic. Let *C*1 be a 1 by 2*N* row vector whose first element is one and the rest are all zero. Then the first harmonic, denoted *vg*1, is *vg*1(*t*) = *C*1*wg*(*t*).

It is easy to verify that the system (4), in particular, the pair (Γ*g, Sg*), is observable. Thus an observer can be constructed to estimate the state *wg*, and hence (*bk, ϕk*) for all *k*. Let the state of the observer be *wz*. We have:

$$\dot{w}_z = S_g w_z - L(\Gamma_g w_z - v_g), \tag{5}$$

Where, L is the observer gain which can be designed via various approaches. A simple approach is to choose the desired poles at −*α* } *jkβ*0, *k* = 1, ・ ・ ・*N* and use the pole placement function in MATLAB. The number *α* can be adjusted via simulation for satisfactory convergence rate.

If the frequency *β*0 for the observer is exactly the same as the frequency of the grid voltage, then the observer error *wz*(*t*) − *wg*(*t*) will go the 0 asymptotically and we can use the estimated state *wz* for various purposes. If the grid frequency is subject to perturbation, this frequency can be measured on line and used for the observer. Due to robustness, the same gain *L* should be stabilizing for a certain range of *β*0 and *Sg*(*β*0). The discrete-time version of the observer are usually used in practice. More details can be found in [40]. With the estimated state *wz*, the first harmonic of *vg* is estimated as *C*1*wz*.

2.3. The Control Objective and Augmented Exosystem

Ideally, we would like to feed the grid a sinusoidal current *ig*, which is in phase with *vg*. The magnitude of *ig* can be varied depending on the need of the grid and the local energy storage devices. This objective can be stated as a reference tracking problem where the reference for the grid current is given as:

$$i_{g,ref}(t) = r v_{g1}(t), \tag{6}$$

Where, *r* is a positive number that can be changed. Recall that *vg*1 is the first harmonic of *vg*.

If *r* is fixed, then the reference *ig;ref* can be considered as another output for the exosystem (4) alongside *vg*. If *r* is variable, it would be more convenient to introduce another exosystem:

$$\dot{w}_r = S_0 w_r, \qquad i_{g,ref} = [1 \quad 0] w_r \tag{7}$$

Where, *wr* ∈**R**2. The condition (6) can be satisfied if *wr*(0) = *rwg*1(0). Since *w*˙ *g*1 = *S*0*wg*1, we have *wr*(*t*) = *rwg*1(*t*). There is some redundancy introducing (7). The purpose is to make it easier to handle *r*.

With the reference current specified, the control objective is to minimize the magnitude of the tracking error.

$$e(t) = i_g(t) - i_{g,ref}(t) \tag{8}$$

At steady state. Note that *ig* can be considered as an output to the inverter system (1): *ig* = [0 0 1]*xc*. Since *B* and *E* in (1) are not aligned, i.e., the control input *u* and the disturbance *vg* are not in the same channel, the tracking error cannot be completely eliminated. In most works on output regulation (e.g., [32-33], [41-42]), similar control problems were considered, but under the assumption that the control input and the disturbance enter the system from the same channel. Under this assumption, part of the control can be used to cancel the disturbance.

Even though the control problem in this work does not fit into the framework of output regulation, we can use the same basic idea of internal model for the disturbance and using an observer to reconstruct the state for an exosystem which produces the disturbance.

The two exosystems (4) and (7) can be stacked up to obtain a 2(*N* + 1) -order system. Define:

$$w = \begin{bmatrix} w_g \\ w_r \end{bmatrix}$$

And,

$$S = \begin{bmatrix} S_g & 0 \\ 0 & S_0 \end{bmatrix}$$
$$\Gamma_1 = [\Gamma_g \quad 0 \quad 0]$$
$$\Gamma_2 = [0 \quad \cdots \quad 0 \quad 1 \quad 0]$$

Then,

$$\dot{w} = Sw, v_g = \Gamma_1 w, i_{g,ref} = \Gamma_2 w$$

This system describes all the dynamics of the grid voltage and the reference current. Combined with the state-space description of the LCL filter, the dynamics of the whole system can be described. Before that, we need to provide some useful properties about the exosystem and some important implications about the initial condition.

It is clear that the exosystem (9) evolves all by itself and is driven by its initial condition *w*(0). Recall that *w* consists of the states for all the harmonics of *vg* and for *ig;ref* , in particular,

$$w = [w_{g1}^T \quad w_{g2}^T \quad \cdots \quad w_{gN}^T \quad w_r^T]^T$$

Since $S + S^T = 0$, we have:

$$w^T(t)w(t) = w^T(0)w(0) = \|w(0)\|^2, \tag{10}$$

$$w_{gk}^T(t)w_{gk}(t) = w_{gk}^T(0)w_{gk}(0) = b_k^2, \tag{11}$$

$$w_r^T(t)w_r(t) = w_r^T(0)w_r(0) = r^2 b_1^2 \tag{12}$$

For all *t*. Thus *//wgk*(0)*//*2 represents the power of the *k*th harmonics of *vg* and *//w*(0)*//*2 the total power of the harmonics of *vg* plus the power of the reference current.

Note that the condition *wr*(*t*) = *rwg*1(*t*) implies that *ig;ref* is proportional to the first harmonic of *vg*. In terms of the combined state *w*, this can be written as:

$$w_1 w_{2N+2} = w_2 w_{2N+1} \tag{13}$$

This condition will be used as a constraint in an optimization problem to be formulated.

3. Lyapunov Approach to Evaluation of the Tracking Error

3.1. Evaluation of Tracking Error for General Exosystem

As we can see from (9), both the grid voltage and the reference current are driven by an autonomous linear system. According to [43], the state variable of an autonomous system contains all the information that determines its future behavior, it can be effectively used to correct the dynamic behavior of the whole system. In the case of the inverter circuit, the state *w* can be used to minimize the tracking error of the grid current (8).

For the inverter circuit in Figure 1, the state of the whole system is a combination of the circuit state*xc* and the exosystem state *w*. They can be either measured or estimated via an

observer, thus state feedback is feasible. In this work, we attempt to use state feedback to minimize the tracking error.

The problem boils down to how to measure the magnitude of the tracking error at steady state? If the tracking error can be effectively evaluated via a certain performance measure, the next step would be minimizing this performance measure via a certain optimization algorithm.

Traditional measures based on transfer function may not be readily applicable to this case. Here we note that the inverter circuit has two exogenous inputs, one is the grid voltage and the other one is the reference current. The grid voltage can be considered as a disturbance whose magnitude is almost fixed, or varies within a small range, but the magnitude of the reference current is variable. Thus it is difficult to use a certain input-output gain to measure the tracking error as the output to these two exogenous inputs. Another difficulty is that there are many harmonics and it is not easy to consider their combined effects.

The Lyapunov approach developed in [31] seems to be tailored for this kind of problems. It deals with more general systems (nonlinear, time-varying) with periodic excitations, which could be disturbance or reference. The objective is to evaluate the magnitude of certain output at steady state, which could be the tracking error.

To apply the Lyapunov approach, we first need the state space description for the whole system, which can be easily obtained by combining the state-space equation (1) for the circuit and the state-space equation (9) for the *vg* and *ig;ref* . Since *ig* = [0 0 1]*xc*, if we let *C* = [0 0 1 − Γ2], then:

$$\begin{bmatrix} \dot{x_c} \\ \dot{w} \end{bmatrix} = \begin{bmatrix} A & E\Gamma_1 \\ 0 & S \end{bmatrix} \begin{bmatrix} x_c \\ w \end{bmatrix} + \begin{bmatrix} B \\ 0 \end{bmatrix} u \tag{14}$$

$$e = C \begin{bmatrix} x_c \\ w \end{bmatrix} \tag{15}$$

To reduce the tracking error, we apply a simple state feedback:

$$u = K_1 x_c + K_2 w = \begin{bmatrix} K_1 & K_2 \end{bmatrix} \begin{bmatrix} x_c \\ w \end{bmatrix} \tag{16}$$

Substitute the feedback law in (16) into (14), we have the closed-loop system.

$$\begin{bmatrix} \dot{x_c} \\ \dot{w} \end{bmatrix} = \begin{bmatrix} A + BK_1 & E\Gamma_1 + BK_2 \\ 0 & S \end{bmatrix} \begin{bmatrix} x_c \\ w \end{bmatrix} \tag{17}$$

$$e = C \begin{bmatrix} x_c \\ w \end{bmatrix} \tag{18}$$

Recall that the dimension of *xc* and *w* are 3 and 2*N* +2, respectively, the order of the whole system is 2*N* +5.

As long as *A* + *BK*1 is stable, the solution for the above system will be bounded and for any initial condition, the solution will approach a steady state oscillation. Since *A* + *BK*1 is stable, the effect of the initial condition of *xc*(0) will vanish asymptotically. Thus the steady state oscillation, in particular, the tracking error, depends only on the initial condition *w*(0). Hence, a gain from the norm of the initial condition $\|w(0)\| = \sqrt{w(0)^T w(0)}$ to the magnitude of *e* at steady state can be defined. The main result of [31] was applied to estimate this gain via a quadratic Lyapunov function $V(x_c, w) = [x_c^T w^T] P \begin{bmatrix} x_c \\ w \end{bmatrix}$.

Here we summarize the main result of the Lyapunov approach when applied to the linear system (17). Denote:

$$A_L(K_1,K_2)=\begin{bmatrix} A+BK_1 & E\Gamma_1+BK_2 \\ 0 & S \end{bmatrix}$$

Theorem 1: For $\gamma > 0$, if there exist a positive definite matrix $P = P^T \in \mathbf{R}^{(2N+5)\times(2N+5)}$, and a number $\eta > 0$ such that:

$$C^TC \le P \tag{19}$$

$$A_L(K_1,K_2)^T P + PA_L(K_1,K_2) \quad \le -\eta\left(P-\gamma\begin{bmatrix} 0 & 0 \\ 0 & I_{2N+2} \end{bmatrix}\right) \tag{20}$$

Where I_{2N+2} is an identity matrix of dimension $2N + 2$, then for any initial condition $x_c(0)$ and $w(0)$, $x_c(t)$ and $e(t)$ will converge to a bounded set. Moreover, the tracking error e at steady state is bounded by $|e(t)| \le \gamma^{\frac{1}{2}}\|w(0)\|$.

The number γ satisfying Theorem 1 is called a bound on the steady state gain from $\|w(0)\|$ to the tracking error e. For given K_1, K_2, this steady state gain can be evaluated by minimizing γ satisfying the LMI constraints (19) and (20), by using the LMI toolbox in Matlab.

Here we note that the norm of the initial condition, $\|w(0)\|^2$, is closely related to the magnitude of v_g and $i_{g,ref}$. To be specific, recall that the state corresponding to the kth harmonic is w_{gk}. Its norm $\|w_{gk}(t)\| = \|w_{gk}(0)\| = b_k$, where b_k is the magnitude of the kth harmonic. Furthermore:

$$\|w(0)\|^2 = \sum_{k=1}^{N}\|w_{gk}\|^2 + r^2w_r^2 = \sum_{k=1}^{N} b_k^2 + r^2b_1^2$$

3.2. Improved Evaluation by Exploring Structural Information

In the previous section, the tracking error was evaluated based on $\|w(0)\|$. Let $\gamma > 0$ satisfy (19) and (20), then at steady state, $|e(t)| \le \gamma^{\frac{1}{2}}\|w(0)\|$. This inequality is valid for all types of $w(0)$ but could be too conservative for a practical grid voltage whose first harmonic dominates the higher order harmonics and for a reference current which is proportional to the first-order harmonic.

In practice, the THD of the grid voltage is below a certain level and the magnitude of the reference current is within a given range. In this section, such structural information will be effectively utilized to improve the evaluation of the tracking error. Specifically, the structural information will be exactly expressed in terms of quadratic inequalities and incorporated in the Lyapunov approach to obtain less restrictive constraints, thus reducing the minimal value of γ for the optimization problem.

1) Quadratic inequality for THD bound: Consider the grid voltage expressed in (2). The THD value is:

$$THD_{v_g} = \frac{(\sum_{k=2}^{\infty} b_k^2)^{\frac{1}{2}}}{b_1}$$

Suppose that a known bound on the THD is ε_0. Then we have:

$$\sum_{k=2}^{\infty} b_k^2 \le \varepsilon_0^2 b_1^2$$

Recall from (11) $b_k^2 = w_{gk}^T(t)w_{gk}(t)$ for all t, the above inequality can be expressed as:

$$\sum_{k=2}^{\infty} w_{gk}^T w_{gk} \le \varepsilon_0^2 w_{g1}^T w_{g1} \tag{21}$$

In terms of the combined state $\begin{bmatrix} x_c \\ w \end{bmatrix}$, this inequality can be expressed as:

$$\begin{bmatrix} x_c^T & w^T \end{bmatrix} W_{THD} \begin{bmatrix} x_c \\ w \end{bmatrix} \geq 0 \tag{22}$$

Where,

$$W_{THD} = \begin{bmatrix} 0_3 & 0 & 0 & 0 \\ 0 & \varepsilon_0^2 I_2 & 0 & 0 \\ 0 & 0 & -I_{2(N-1)} & 0 \\ 0 & 0 & 0 & 0_2 \end{bmatrix}$$

And 0*p* denotes a *p* × *p* 0 block and other 0's have compatible dimensions.

2) Quadratic inequality for magnitude of reference current: The reference current is proportional to the first harmonic *vg*1 and is set as *i*2;*ref* (*t*) = *rvg*1(*t*). Suppose that *r* is bounded by *rmax*. Then we have $w_r^T w_r \leq r_{max}^2 w_{g1}^T w_{g1}$. In terms of $\begin{bmatrix} x_c \\ w \end{bmatrix}$, this constraint can be written as:

$$\begin{bmatrix} x_c^T & w^T \end{bmatrix} W_{rm} \begin{bmatrix} x_c \\ w \end{bmatrix} \geq 0 \tag{23}$$

Where *Wrm* is given by:

$$W_{rm} = \begin{bmatrix} 0_3 & 0 & 0 & 0 \\ 0 & r_{max}^2 I_2 & 0 & 0 \\ 0 & 0 & 0 & 0 \\ 0 & 0 & 0 & -I_2 \end{bmatrix}$$

3) Quadratic equality for phase of reference current: The reference current is in phase with the first harmonic *vg*1. This implies that the state *wr* is proportional to the state *wg*1. Let $w_r = \begin{bmatrix} w_{r,1} \\ w_{r,2} \end{bmatrix}$, $w_{g1} = \begin{bmatrix} w_{g1,1} \\ w_{g1,2} \end{bmatrix}$. Then:

$$w_{r,1} w_{g1,2} = w_{r,2} w_{g1,1}$$

In terms of the whole state, this is equivalent to:

$$\begin{bmatrix} x_c^T & w^T \end{bmatrix} W_{rp} \begin{bmatrix} x_c \\ w \end{bmatrix} = 0 \tag{24}$$

Where *Wrp* is given by:

$$W_{rp} = \begin{bmatrix} 0_3 & 0 & 0 & 0 \\ 0 & 0_2 & 0 & \begin{bmatrix} 0 & 1 \\ -1 & 0 \end{bmatrix} \\ 0 & 0 & 0_{2(N-1)} & 0 \\ 0 & \begin{bmatrix} 0 & -1 \\ 1 & 0 \end{bmatrix} & 0 & 0_2 \end{bmatrix}$$

Now we can use the quadratic inequalities (22), (23) and (24) to improve the evaluation of the tracking error.

Corollary 1: Consider the closed loop system (17). Suppose that the THD of the grid voltage is less than ε0 and *ig;ref* (*t*) = *rvg*1(*t*) with *r* ≤ *rmax*. For *γ* > 0, if there exist a positive definite matrix *P* = *PT* ∈**R**(2*N*+5)_(2*N*+5), and number *η, α*1*, α*2 ≥ 0, *α*3 ∈**R** such that:

$$C^T C \leq P \tag{25}$$

$$A_L(K_1,K_2)^T P + P A_L(K_1,K_2) \leq -\eta \left(P - \gamma \begin{bmatrix} 0 & 0 \\ 0 & I_{2N+2} \end{bmatrix} \right) - \alpha_1 W_{THD} - \alpha_2 W_{rm} - \alpha_3 W_{rp}, \tag{26}$$

Where *I*2*N*+2 is an identity matrix of dimension 2*N* + 2, then for any initial condition *xc*(0) and *w*(0), *xc*(*t*) and *e*(*t*) will converge to a bounded set. Moreover, the tracking error *e* at steady state is bounded by:

$$|e(t)| \leq \gamma^{\frac{1}{2}} (b_1^2 + \cdots + b_N^2 + r^2 b_1^2)^{\frac{1}{2}}$$

Proof: Due to linearity of the system (17), we can consider *w*(0) such that $\|w(0)\| \leq 1$. We need to prove that $|e(t)| \leq \gamma^{\frac{1}{2}}$ at steady state. Note that $\|w(0)\| = (b_1^2 + \cdot + b_N^2 + r^2 b_1^2)^{\frac{1}{2}}$.

For simplicity, denote $\xi = \begin{bmatrix} x_c \\ w \end{bmatrix}$. Consider the quadratic Lyapunov function $V(\xi) = \xi^T P \xi$. Its *γ* level set is:

$$\mathcal{E}(P,\gamma) = \{\xi \in \mathbf{R}^{(2N+5)} : \xi^T P \xi \leq \gamma\}$$

Which is an ellipsoid. The condition (25) implies that [44]:

$$|e(t)| = |C\xi| \leq \gamma^{\frac{1}{2}} \text{ for all } \xi \in \mathcal{E}(P,\gamma)$$

It suffices to show that under $\|w(0)\| \leq 1$, the state *ξ* will converge to *E*(*P, γ*). This is guaranteed if *V* (*ξ*(*t*)) is strictly decreasing, i.e., ˙*V* (*ξ*) < 0, as long as *V* (*ξ*) ≥ *γ*. We use the condition (26) to prove this. For the system (17), we have:

$$\dot{V}(\xi) = \xi^T (A_L(K_1,K_2)^T P + P A_L(K_1,K_2)) \xi$$

Thus condition (26) implies that:

$$\dot{V}(\xi) < -\eta \xi^T \left(P - \gamma \begin{bmatrix} 0 & 0 \\ 0 & I_{2N+2} \end{bmatrix} \right) \xi - \xi^T (\alpha_1 W_{THD} + \alpha_2 W_{rm} + \alpha_3 W_{rp}) \xi$$

By the structural information (22)-(24) and *α*1*, α*2 ≥ 0, we have:

$$-\xi^T (\alpha_1 W_{THD} + \alpha_2 W_{rm} + \alpha_3 W_{rp}) \xi \leq 0$$

Since $\|w(0)\| \leq 1$, we have $w(t)^T w(t) \leq 1$ for all *t*, i.e., $\xi^T \begin{bmatrix} 0 & 0 \\ 0 & I_{2N+2} \end{bmatrix} \xi \leq 1$. Therefore,

$$\dot{V}(\xi) < -\eta (V(\xi) - \gamma)$$

Which implies that *V* (*ξ*(*t*)) is strictly decreasing as long as *V* (*ξ*(*t*)) ≥ *γ*. This completes the proof.

The constraint (26) is less restrictive than the corresponding condition (20) due to the additional parameters *α*1*, α*2*, α*3 in the terms −*α*1*WTHD,*−*α*2*Wrm* and −*α*3*Wrp*, which result

from the structural information. The effectiveness of each additional term will be demonstrated via computation results.

For given feedback gain *K*1,*K*2, the magnitude of the tracking error *e* can be evaluated by solving an optimization problem with matrix inequality constraints.

4. Design of State-feedback Law Via Lmi-based Optimization

The analysis problem in the previous section can be readily turned into a design problem by considering *K*1, *K*2 as additional optimization parameters. Putting everything together, we have the following optimization problem.

$$\inf_{P,K_1,K_2,\eta,\alpha_1,\alpha_2,\alpha_3} \quad \gamma \tag{27}$$

$$\begin{aligned}
\text{s.t} \quad & a) \;\; C^T C \le P \\
& b) \;\; A_L(K_1,K_2)^T P + P A_L(K_1,K_2) \\
& \quad \le -\eta \left(P - \gamma \begin{bmatrix} 0 & 0 \\ 0 & I_{2N+2} \end{bmatrix} \right) \\
& \quad - \alpha_1 W_{THD} - \alpha_2 W_{rm} - \alpha_3 W_{rp} \\
& c) \;\; P > 0, \alpha_1, \alpha_2, \eta > 0
\end{aligned}$$

When *K*1,*K*2 are considered as optimization parameter, the above optimization problem has bilinear terms in constraint b). We may use the path-following method as used in [45] to find the optimal or sub-optimal solution.

5. Computation and Simulation Results

We constructed the Simulink model for the inverter using SimPower in Matlab. The model is included a transistor bridge controlled by PWM signals. The parameters for the circuit in Figure 1 are given as follows: *Lf* = 150*μH*, *Lg* = 450*μH*, *Cf* = 22*μF*, *Rf* = 0.02Ω, *Rg* = 0.02Ω, *Rd* = 1Ω.

The switching frequency is 20KHz and the DC voltage supply is 12V. The state feedback is processed by a low pass filter $\frac{1}{1+s\frac{1}{3000}}$ before sent to drive the transistor bridge.

The grid voltage *vg* was measured via a transformer and its harmonic components were analyzed with Matlab.

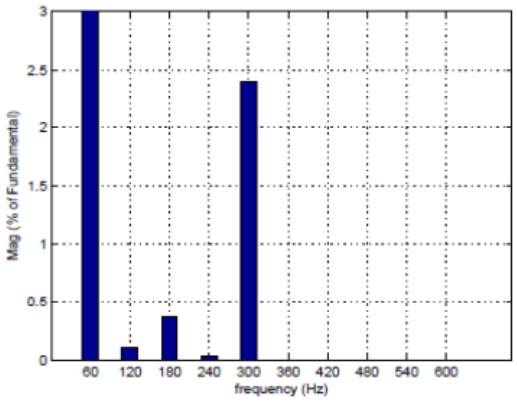

Figure 2. Hamonic Components of Grid Voltage

Figure 2 is the grid voltage harmonic components. Its fundamental frequency is $\beta 0 = 60Hz$. The total harmonic distortion (THD) is 2.434%. For simulation, only the first 5 harmonics are kept. The resulting *vg* used for simulation is:

$vg(t) = 7.9554\sin(\beta 0t - 0.4868) + 0.0084\sin(2\beta 0t - 0.5250) + 0.0299\sin(3\beta 0t + 2.6702) + 0.0032\sin(4\beta 0t - 1.1385) + 0.1911\sin(5\beta 0t + 0.3363)$

The reference current is $ig;ref = r7.9554sin(\beta 0t - 0.4868)$, with *r* is the proportional factor. In this simulation, $r = 0.2$. The output current *ig* will be created in proportion with *ig;ref* .

By choosing different weighting for K, and solving the optimization problem, we obtained the feedback gain K.

K = [-0.2005 7.1971 -72.8533 0.2944 -0.0012 0.2942 -0.0023 0.2940 -0.0035 0.2936 -0.0046 0.2932 -0.0058 1.3568 0.0545]

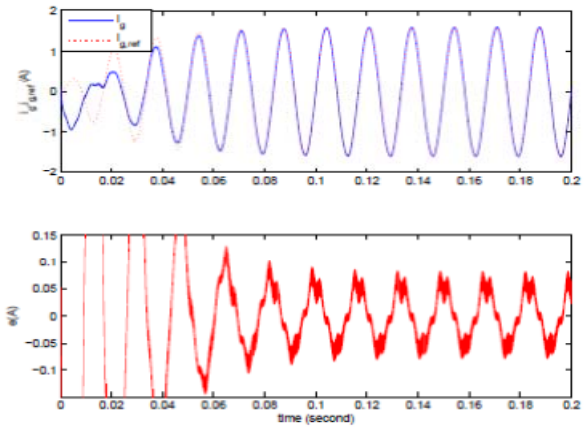

Figure 3. Grid Current *ig* and Tracking Error by PWM Model

Figure 3 shows the tracking performance by the PWM model. The magnitude of tracking error at stable state is 0.08(A) and the THD value for *ig* is 0.9369%. Figure 4 shows the harmonic components of the current output *ig*.

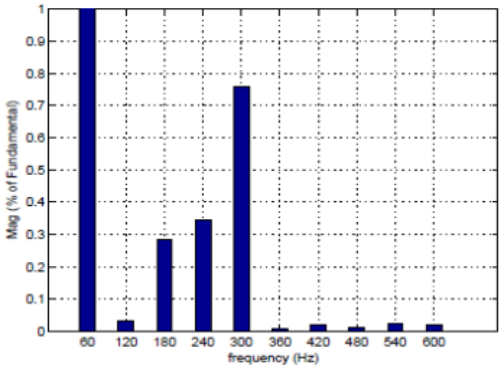

Figure 4. Harmonic Components of the Current Output *ig*

6. Experimental Results

We built an experimental DC-AC inverter as in Figure 1. The parameters for the real circuit are given as follows: $Lf = 150\mu H$, $Lg = 450\mu H$, $Cf = 22\mu F$, $Rf = 0.045\Omega$, $Rg = 0.135\Omega$, $Rd = 1\Omega$. The DC supply voltage is $Vs = 12V$. The MOSFETs bridge is driven by PWM signal.

The control module is implemented in digital domain by using Texas Instruments TMS320F28335. The main features of this DSP is 150MHz operating speed, 16 input channels (12-bit ADC), and up to 18 PWM outputs. The ADC input receives analog signals and converts them into digital signals. The operating range of analog input signals is from 0V to 3V. So the state feedback signals are scaled to the range between 0V and 3V before sending to the inputs of DSP to maximize the resolution and prevent the DSP from over-limited voltage. The PWM signal taken from DSP output is programmed at 18kHz switching frequency.

The grid voltage *vg* is observed by the controller via a step-down transformer, which has 60Hz frequency. The reference tracking problem is validated with three different values of *r* = 0.2, 0.3, and 0.4, as in Figure 5, 6 and 7.

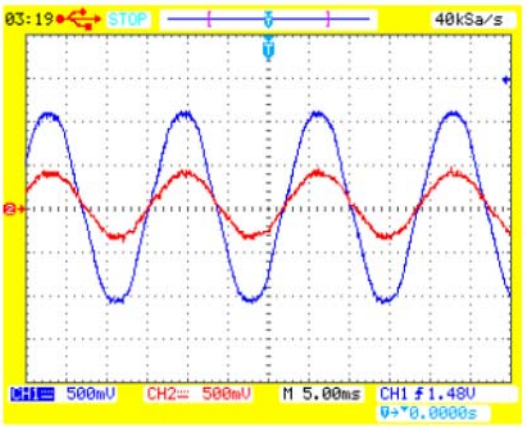

Figure 5. Grid Voltage and Current Output with *r* = 0.2

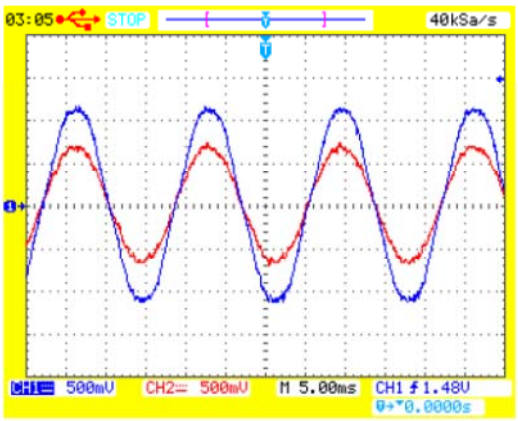

Figure 6. Grid Voltage and Current Output with *r* = 0.3

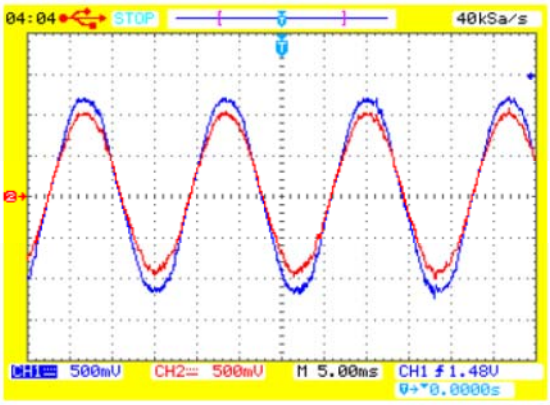

Figure 7. Grid Voltage and Current Output with *r* = 0.4

Figure 5, 6, 7 show the grid voltage that was stepped down by the transformer and the grid current with *r* = 0.2, 0.3, and 0.4. The blue curve is the voltage from transformer, its value is 5V. In the figure, it was scaled down 5 times. The red curve is the current to transformer. It was measured on the current sense 0.1Ω, then scaled up 10/2.4 = 4.16 times. In Figure 5, the real value of the current should be (400*mV*/4.16)/0.1Ω = 960*mA*. In Figure 6, the real value of the current should be (700*mV*/4.16)/0.1Ω = 1680*mA*. In Figure 7, the real value of the current should be (1000*mV*/4.16)/0.1Ω = 2400*mA*.

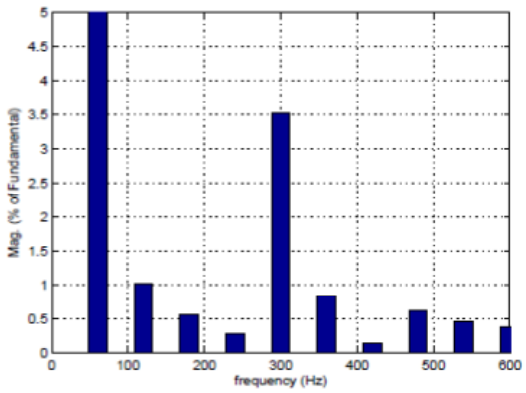

Figure 8. Spectrum of the Current with r = 0.2

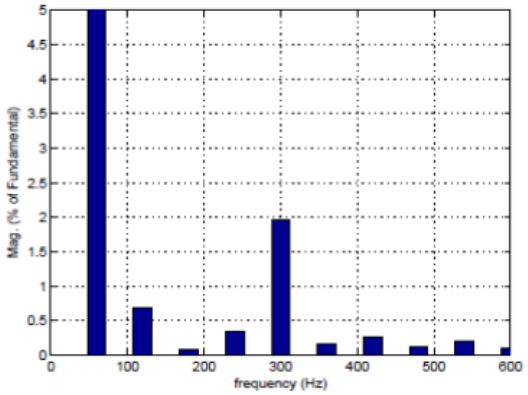

Figure 9. Spectrum of the Current with r = 0.3

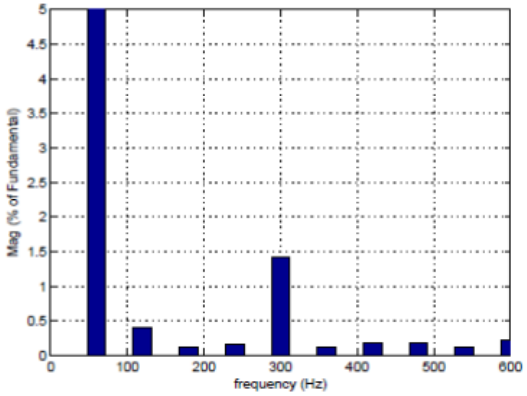

Figure 10. Spectrum of the Current with r = 0.4

Figure 8, 9, 10 show the harmonic components of the corresponding currents. The fundamental frequency is 60Hz.

Table 1. Harmonics of current with r = 0.2, 0.3 and 0.4

r	Fundamental (60Hz)	*2nd*	*3rd*	*4th*	*5th*
0.2	0.3661	0.0037	0.0021	0.0011	0.0129
0.3	0.6756	0.0046	0.0005	0.0023	0.0133
0.4	0.9704	0.0039	0.0011	0.0015	0.0138

The current magnitudes of fundamental frequency and its harmonics are presented in the Table 1 for difference values of r. The THDs of the current calculated for 10 harmonics are 3.9269%, 2.1514%, and 1.542% corresponding with r = 0.2, 0.3, and 0.4.

7. Conclusion

This paper developed a Lyapunov approach to modeling and design, the state-feedback control for grid-connected inverters. The method was applicable to inverters connected to the grid via a transformer. The model ensures the internal stability and makes efficient use of harmonic information of the grid voltage, and the magnitude/phase of the reference current. The effectiveness of this design was then validated by SimPower simulation. A real circuit was built using DSP TMS320F28335 to verify the design. The results show the robustness of the design, the output of the inverter can be fed to the grid with low THD.

References

[1] S Kjaer, J Pedersenm, F Blaab jerg. A Review of Single-Phase Grid-Connected Inverters for Photo- voltaic Modules. *IEEE Trans. on Industry Applications.* 2005; 41(5): 1292-1306.

[2] B Li, MM Zhang, L Huang, L Hang, LM Tolbert. A robust multi-resonant PR regulator for three-phase grid-connected VSI using direct pole placement design strategy. *Applied Power Electronics Conference and Exposition (APEC)*. 2013; 45(6): 960 - 966.

[3] GG Pozzebon, AFQ Goncalves, GG Pena, NEM Mocabique, RQ Machado. Operation ofThree-Phase Power Converter Connected to a Distribution System. *IEEE Transactions on Industry Electronics*. 2013; 60(5): 1810-1818.

[4] X Chen, YH Wang, YC Wang. A novel seamless transferring control method for microgrid based on master-slave configuration. *ECCE Asia Downunder (ECCE Asia). IEEE*. 2013: 351 - 357.

[5] Z Yao, L Xiao, Y Yan. Seamless Transfer of Single-Phase Grid-Interactive Inverters Between Grid-Connected and Stand-Alone Modes. *IEEE Trans. on Power Electronics.* 2010; 25(6): 1597-1603.

[6] P Piagi, RH Lasster. Autonomous control of microgrids. *Proceeding of 2006 IEEE Power Engineering Society General Meeting. Montreal, Quebec, Canada*. 2006; 8-15.

[7] Y Ye, B Zhang, K Zhou, D Wang, Y Wang. High-performance cascade-type repetitive controller for CVCF PWM inverter: analysis and design. *IET Electric Power Applications*. 2007; 1(1): 112-118.

[8] Y Ye, B Zhang, K Zhou, D Wang, J Wang. High-Performance Repetitive Control of PWM DC-AC Converters With Real-Time Phase-Lead FIR Filter. *IEEE Transactions on Circuits and Systems*. 2006; 53(8): 768-772.

[9] S Chen, YM Lai, SC Tan, CK Tse. Analysis and design of repetitive controller for harmonic elimina- tion in PWM voltage source inverter systems. *IET Electric Power Applications*. 2008; 1(4): 497-506.

[10] YY Tzou, SL Jung, HC Yeh. Adaptive Repetitive Control of PWM Inverters for Very Low THD AC-Voltage Regulation with Unknown Loads. *IEEE Transactions on Power Electronics*. 1999; 14(5): 973-981.

[11] K Zhou, D Wang, B Zhang, Y Wang. Plug-In Dual-Mode-Structure Repetitive Controller for CVCF PWM Inverters. *IEEE Trans. on Industrial Electronics*. 2009; 56(3): 784-791.

[12] G Weiss, QC Zhong, TC Green, J Liang. "H^{∞}Repetitive Control of DC-AC Converters in Microgrids. *IEEE Trans. on Power Electronics*. 2004; 19(1): 219-230.

[13] T Hornik. QC Zhong. A Current-Control Strategy for Voltage-Source Inverters in Microgrids Based on $H^{\infty}$and Repetitive Control. *IEEE Transactions on Power Electronics*. 2011; 26(3): 943-952.

[14] D Chen, J Zhang, Z Qian. An Improved Repetitive Control Scheme for Grid-Connected Inverter with Frequency-Adaptive Capability. *IEEE Trans. on Industrial Electronics*. 2013; 60(2): 814 -823.

[15] A Garca-Cerrada, O Pinzn-Ardila, V Feliu-Batlle, P Roncero-Snchez, P Garca-Gonzlez. Application of a Repetitive Controller for a Three-Phase Active Power Filter. *IEEE Transactions on Power Electronics*. 2007; 22(1): 237-246.

[16] R Costa-Castello, R Grino, R Cardoner Parpal, E Fossas. High Performance Control of a Single-Phase Shunt Active Filter. *IEEE Trans. on Control Systems Technology*. 2009; 17(6): 1318-1329.

[17] M Routimo, M Salo, H Tuusa. Comparison of Voltage-Source and Current-Source Shunt Active Filters. *IEEE Transactions on Power Electronics*. 2007; 22(2): 636 - 643.

[18] T Fujii, T Yokoyama. FPGA based Deadbeat Control with Disturbance Compensator for Single Phase PWM Inverter. *Proc. IEEE Power Electronics Specialists Conference.* 2006; 1-6.

[19] P Mattavelli. An improved deadbeat control for UPS using disturbance observers. *IEEE Transactions on Industry Electronics*. 2005; 52(1): 206-212.

[20] QC Zhong. Harmonic Droop Controller to Reduce the Voltage Harmonics of Inverters. *IEEE Trans- actions on Industry Applications*. 2013; 60(3): 936-945.

[21] R Teodorescu, F Blaab jerg, M Liserre, PC Loh. Proportional resonant controllers and filters for grid-connected voltage-source converters. *IEE Proc. Electric Power Applications*. 2006; 153(5): 750-762.

[22] C Lascu, L Asiminoaei, I Boldea, F Blaab jerg. High Performance Current Controller for Selective Harmonic Compensation in Active Power Filters. *IEEE Transactions on Power Electronics*. 2007; 22(5): 1826-1835.

[23] Z Shicheng, W Peizhen, G Lusheng. *Study on improving output current waveform of photovoltaic grid-connected system.* IEEE Conference on Industrial Electronics and Applications. 2006.

[24] X Wang, M Kazerani. A multicarrier modular photovoltaic grid-connected inverter with a new phase-shift rule. *Electric Power Systems Research*. 2007; 754 -760.

[25] F Blaab jerg, R Teodorescu, M Liserre, AV Timbus. Overview of control and grid synchroniza- tion for distributed power generation systems. *IEEE Trans. On Indust. Elect.*, 2006; 53(5): 1398-1409.

[26] J He, G Zhao. The Simulation of Controlling Strategy for Output Current Tracking of Grid-connected Inverter. *IEEE Symposium on Electrical & Electronics Engineering*. 2012; 171-174.

[27] X Jin. Photovoltaic Grid connected Inverter Harmonic Compensation and Grid-connected Unified Control. *Power and Energy Engineering Conference, Asia-Pacific*. 2009; 1-4.

[28] W Haibo, C Yanbo, Z Lihua. *Research and Development of Photovoltaic Grid-connected Inverter Based on DSP.* International Conference on Power Electronics Systems and Applications (PESA). 2011; 1-5.
[29] Y Xiong, S Qian, J Xu. *Single-phase grid-connected photovoltaic system based on boost inverter*. Power and Energy Engineering Conference (APPEEC). 2012; 1-3.
[30] Y Yang, K Zhou, F Blaab jerg. *Harmonics suppression for single-phase grid-connected PV systems in different operation modes*. Applied Power Electronics Conference and Exposition (APEC). 2013; 889-896.
[31] T Hu, AR Teel, Z Lin. Lyapunov characterization of forced oscillations. *Automatica*. 2005; 1723-1735.
[32] T Hu, Z Lin. Output regulation of linear systems with bounded continuous feedback. *IEEE Trans. Automatic Control*. 2004; 1941-1953.
[33] A Isidori, CI Byrnes. Output Regulation of Nonlinear Systems. *IEEE Trans on Automatic Control.* 1990; 35: 131-140.
[34] Y Yao, F Fassinou, T Hu. Stability and Robust Regulation of Battery Driven Boost Converter with Simple Feedback. *IEEE Trans. On Power Electronics*. 2011; 2614-2626.
[35] H Pham, H Jung, T Hu. State-Space Approach to Modeling and Ripple Reduction in AC-DC Converters. *IEEE Trans. on Control Systems Technology*. 2013; 21(5): 1949-1955.
[36] RW Erickson, D Maksimovic. *Fundamentals of Power Electronics*, 2nd edition, Springer. 2001.
[37] G Escobar, AA Valdez, J Leyva-Ramos, P Mattavelli. Repetitive Based Controller for a UPS Inverter to Compensate Unbalance and Harmonic Distortion. *IEEE Trans. Industrial Electronics*. 2007; 54(1): 504-510.
[38] S Fukuda, R Imamura. Application of a Sinusoidal Internal Model to Current Control of Three-phase Utility-Interface Converters. *IEEE Trans. on Industrial Electronics*. 2005; 52(2): 420-426.
[39] K Lee, TM Jahns, TA Lipo, V Blasko, RD Lorenz. Observer-Based Control Methods for Combined Source-Voltage Harmonics and Unbalance Disturbances in PWM Voltage-Source Converters. *IEEE Transactions on Industry Applications*. 2009; 45(6): 2010-2021.
[40] K Selvajyothi, PA Janakiraman. Extraction of Harmonics Using Composite Observers. *IEEE Trans. Power Delivery*. 2008; 23(1): 31-40.
[41] BA Francis. The Linear Multivariable regulator Problem. *SIAM Journal of Control and Optimization.* 1977; 15: 486-505.
[42] B Francis, W Wonham. The Internal Model Principle for Linear Multivariable Regulators. *Appl. Math. Optimization*. 1975; 2: 170-194.
[43] CT Chen. *Linear System Theory and Design*, 3rd edition. Oxford University Press. 1998.
[44] S Boyd, L El Ghaoui, E Feron, V Balakrishnan. Linear Matrix Inequalities in System and Control Theory. Philadelphia: *SIAM Studies in Applied Mathematics.* 1994.
[45] T Hu. Conjugate Lyapunov Functions for saturated Linear Systems. *Automatica*. 2005; 41(11): 1949-1956.